

CHAPTER 14

NEW DEVELOPMENTS IN TOPOLOGICAL FLUID MECHANICS: FROM KELVIN'S VORTEX KNOTS TO MAGNETIC KNOTS

RENZO L. RICCA

*Department of Mathematics, University College London,
Gower Street, London WC1E 6BT, UK*

and

*ISIS, TP 723, EC Joint Research Centre,
21020 Ispra (VA), Italy*

E-mail: ricca@math.ucl.ac.uk

In this paper we review classical and new results in topological fluid mechanics based on applications of first principles of ideal fluid mechanics and knot theory to vortex and magnetic knots. After some brief historical remarks on the first original contributions to topological fluid mechanics, we review basic concepts of topological fluid mechanics and local actions of fluid flows. We review some classical, but little known, results of J.J. Thomson on vortex links, and discuss Kelvin's conjecture on vortex knots. In the context of the localized induction approximation for vortex motion, we present new results on existence and stability of vortex filaments in the shape of torus knots. We also discuss new results on inflexional magnetic knots and possible relaxation to minimal braids. These results have potentially important applications in disciplines such as astrophysics and fusion plasma physics.

1 Kelvin's vortex atoms and the origin of topological fluid mechanics

The use of topological ideas in fluid mechanics dates from the original studies of Gauss^{7,5} on linked orbits and electric circuits, from Lord Kelvin's¹³⁻¹⁴ first investigations on vortex knots, and from Maxwell's¹⁹ thoughts on magnetic flux tubes (see the table in Figure 1 below).

Gauss's work was followed by the studies of Listing on topological properties of surfaces (among which the famous one-sided band, wrongly attributed to Möbius), and by the work of Riemann on analytic properties of irrotational flows embedded in multiply connected regions (with applications to fluid flows in presence of holes).

But it was Kelvin (then W. Thompson), who gave the greatest impetus to applications of topological ideas to physics. His work was inspired by Helmholtz's⁹ influential paper on vortex motion, and was motivated by the search for a fundamental theory of matter. Kelvin's theory assumed the existence of a dynamical fluid ether permeating everything, in which natural forces were generated. Kelvin's realization that vortex filaments in inviscid fluid were

Linking number formula (C.F. Gauss, 1833)	Applications to vector fields (J.C. Maxwell, 1873)
Classification of knots (P.G. Tait, 1867)	Applications to vortices (Lord Kelvin, 1867)

Figure 1: First contributions to the origin of topological fluid mechanics.

permanent, dynamical entities, led him to envisage a vortex atom theory¹³, whose fundamental constituents, the atoms, were knotted vortices embedded in the ether. In absence of dissipation the topology of vortex structures, given for example by the linking of two vortices, is frozen in the fluid, so that knotted and linked structures remain knotted and linked indefinitely. For Kelvin the topological specificity of each knot and link type provided a useful paradigm to represent chemical elements and compounds. By interpreting knotted vortices as elemental building blocks, and links as compounds, it was possible to envisage chemical structures ordered in a way similar to the modern periodic table of elements. The puzzle of quantization of energy, revealed by the spectral studies of light, could thus find a simple and natural explanation in terms of the discrete specificity of the knot types. These ideas became part of a topological theory of matter³² *ante-litteram*. The mathematical study of knots and links thus became an integral part of Kelvin's programme, and this study was carried out by his friend and collaborator Tait. The results of Tait's work,³⁵ that included the first classification tables of knots, were published in a series of three remarkable papers destined to become the foundations of modern knot theory.

Other contributions followed soon. Most notably the work of J.J. Thomson³⁶ on vortex links (see Section 3 below) and the studies of fluid flows in multiply connected domains (see, for example, Lamb's Hydrodynamics¹⁶). These ideas survived for some time. In Lichtenstein's mathematical theory of hydrodynamics,¹⁸ for example, the importance of topology is emphatically stressed by two chapters dedicated to the subject.

While Kelvin's dream of explaining atoms as knotted vortices in a fluid ether never came to fruition, his work was seminal in the development of topological fluid mechanics. The recent revival is mainly due to the work of Moffatt,²⁰ on topological interpretation of helicity, and Arnold,¹ on asymptotic linking number of space-filling curves. Modern developments have been influ-

enced by the recent progress in the theory of knots and links, and by access to fast computer and sophisticated numerical diagnostics. Various research areas now benefit from use of topological techniques and fluid mechanics (an overview of the present state of the art is given, for example, by the article of Ricca & Berger³⁰).

We list here some current research topics relevant to topological fluid mechanics:²²

- *Knotted and linked solutions to Euler's equations:*
 - topological classification of fluid flows;
 - relationships between topology and dynamics;
 - rôle of invariants and integrability;
 - relationships between topology and stability properties.
- *Energy relaxation for topologically complex structures:*
 - magnetic knots and braids;
 - electrically charged links;
 - relationships between topology and energy;
 - energy spectra for physical knots and links.
- *Dynamical systems and measure-preserving flows:*
 - existence theorems for 3-D vector fields;
 - topologically complex closed and chaotic orbits;
 - relationships between topology and Hamiltonian flows;
 - Lie-algebras of invariants.
- *Change of topology and complexity measures:*
 - singularity formation;
 - bifurcation theory and classification of singularities;
 - physical reconnection mechanisms;
 - measures of topological complexity and diagnostics.

2 Basic concepts in topological fluid mechanics

2.1 Topological equivalence classes for frozen fields

We consider an ideal and perfectly conducting fluid in an infinite domain \mathcal{D} of \mathbb{R}^3 . Motion of fluid particles is given by a smooth velocity field $\mathbf{u} = \mathbf{u}(\mathbf{X}, t)$, where \mathbf{X} denotes the position vector and t time. The velocity field satisfies the solenoidal condition in \mathcal{D} and the condition to be at rest at infinity:

$$\nabla \cdot \mathbf{u} = 0 \quad , \quad \text{in } \mathcal{D} \quad , \quad (1)$$

$$\mathbf{u} = 0 \quad , \quad \text{as } \mathbf{X} \rightarrow \infty \quad . \quad (2)$$

Fluid particles move in \mathcal{D} from one position to another. If $\mathbf{a} = \mathbf{X}(\mathbf{a}, 0)$ denotes the initial position of a fluid particle at time $t = 0$, then we have a flow map φ_t induced by \mathbf{u} so that each particle at the initial position \mathbf{a} and time $t = 0$ is sent to the final position $\mathbf{X}(\mathbf{a}, t)$ by

$$\varphi_t : \mathbf{a} \rightarrow \mathbf{X} \quad , \quad \forall t \in I \quad , \quad (3)$$

where I denotes some finite time interval. The flow map φ is continuous, one-to-one and onto, with inverse. For an incompressible fluid the flow map is volume preserving, with Jacobian

$$J = \det \left(\frac{\partial X_i}{\partial a_j} \right) = 1 \quad . \quad (4)$$

Let $\boldsymbol{\Omega} = \boldsymbol{\Omega}(\mathbf{X}, t)$ be a solenoidal ($\nabla \cdot \boldsymbol{\Omega} = 0$) vector field in the fluid domain \mathcal{D} . Then, the evolution of the vector field $\boldsymbol{\Omega}$ is governed by the following master equation:

$$\frac{\partial \boldsymbol{\Omega}}{\partial t} = \nabla \times (\mathbf{u} \times \boldsymbol{\Omega}) \quad . \quad (5)$$

If $\boldsymbol{\Omega}$ is the vorticity $\boldsymbol{\omega} = \nabla \times \mathbf{u}$, eq. (5) is the Helmholtz equation for the transport of vorticity in ideal fluids (Euler's equations). Alternatively, if $\boldsymbol{\Omega}$ is the magnetic field \mathbf{B} , then eq. (5) governs the evolution of \mathbf{B} in ideal magnetohydrodynamics (MHD). Equation (5) admits formal integral solutions called Cauchy equations, given by

$$\boldsymbol{\Omega}(\mathbf{X}, t) = \boldsymbol{\Omega}(\mathbf{a}, 0) \cdot \frac{\partial}{\partial \mathbf{a}} \mathbf{X} = \Omega_j \frac{\partial X_i}{\partial a_j} \quad , \quad (6)$$

that conserve topology. This means that while the field geometry changes smoothly from one configuration to another by continuous actions of flow maps,

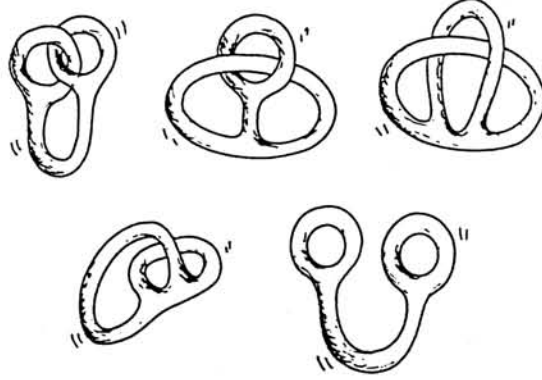


Figure 2: Topologically equivalent configurations of a fluid pretzel.

the initial field topology is conserved. Equation (6) encapsulates both the convection of the field from the initial position \mathbf{a} to the final position \mathbf{X} , and the simultaneous rotation and distortion of fluid elements by the deformation tensor $\partial X_i / \partial a_j$. Since this tensor is a time-dependent diffeomorphism of positions, it maps continuously the initial field distribution $\Omega(\mathbf{a}, 0)$ to $\Omega(\mathbf{X}, t)$ by establishing a topological equivalence between the two fields. Hence, we write

$$\Omega(\mathbf{a}, 0) \sim \Omega(\mathbf{X}, t). \quad (7)$$

Under these conditions the field Ω is said to be 'frozen' in the fluid and initial and final configurations are said to be isotopic to each other.

Continuous deformations of fluid structures are often complicated by twisting and folding actions of fluid flows. The five configurations of a fluid pretzel shown in Figure 2 provide a striking example of equivalent isotopies of a fluid structure by (non-trivial) flow maps.

2.2 Action of local flows and Reidemeister's moves

Ideal topological fluid mechanics deals essentially with the study of fluid structures that are continuously deformed from one configuration to another by ambient isotopies. Since the fluid flow map φ is both continuous and invertible, then $\varphi_{t_1}(\mathcal{K})$ and $\varphi_{t_2}(\mathcal{K})$ generate isotopies of a fluid structure \mathcal{K} (for example a vortex filament) for any $\{t_1, t_2\} \in I$. Isotopic flows generate equivalence classes of (linked and knotted) fluid structures. In the case of (vortex

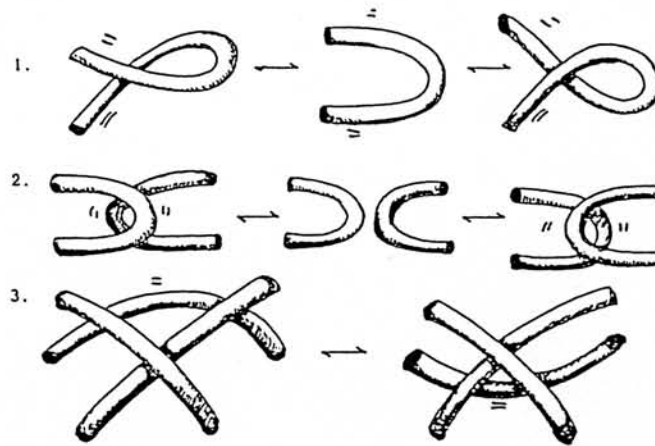


Figure 3: The three types of Reidemeister's moves can be performed by natural actions of local fluid flows on fluid flux tube strands.

or magnetic) fluid flux tubes, fluid actions induce continuous deformations in \mathcal{D} . One of the simplest deformations is local stretching of the tube. From a mathematical viewpoint this deformation corresponds to a time-dependent, continuous re-parametrization of the tube centreline. This re-parametrization (via homotopy classes) generates ambient isotopies of the flux tube, with a continuous deformation of the integral curves.

It is well known (see, for example, Kauffman¹¹) that knot topology is conserved under the action of the Reidemeister moves (see Figure 3). In the context of the Euler equations these moves are performed quite naturally by the action of local flows on flux tube strands. If the fluid in $(\mathcal{D} - \mathcal{K})$ is irrotational, then these fluid flows (with velocity \mathbf{u}) must satisfy the Dirichlet problem for the Laplacian of the stream function ψ , that is

$$\left. \begin{array}{l} \mathbf{u} = \nabla \psi \\ \nabla^2 \psi = 0 \end{array} \right\} \quad \text{in } (\mathcal{D} - \mathcal{K}), \quad (8)$$

with normal component of the velocity to the tube boundary \mathbf{u}_\perp given. Equations (8) admit a unique solution in terms of local flows,² and these flows are interpretable in terms of Reidemeister's moves performed on the tube strands. Note that boundary conditions prescribe only \mathbf{u}_\perp , whereas no condition is im-

posed on the tangential component of the velocity. This is consistent with the fact that tangential effects do not alter the topology of the physical knot (or link). The three types of Reidemeister's moves are therefore performed by local fluid flows, which are solutions to (8), up to arbitrary tangential actions.

2.3 *Ideal versus 'real' topological fluid mechanics*

Relationships between topology and dynamics of fluid structures are very little explored. Questions about topology and dynamics or stability of linked vortices, topology and energy levels of magnetic loops, or energy relaxation of knotted magnetic fields, are still very little studied.

In ideal conditions (i.e. in absence of dissipative effects) all topological properties and physical quantities are conserved. These form a set of scalar and vector invariants that guide the evolution of the system towards (homotopic) solutions, whose existence is guaranteed by the diffeomorphisms associated with the flow maps. Changes in the topology of the system occur only if singularities, bifurcations and dissipative effects are present. Clearly, if we want to model 'real' flow maps, then we cannot neglect the presence of wakes, boundary layers and other fluid regions, where dissipative effects are indeed relevant. Similarly, we cannot neglect the presence of physical regions, where particle trajectories have wild behaviours, with bifurcations, multiple points and singularities. In neglecting the presence of these physical regions we are in fact limiting the validity of the models. Results obtained by techniques of ideal topological fluid mechanics (where dissipative effects are ignored) should therefore be preliminary to the study of real flows, but then complemented or adjusted by 'real' fluid mechanics.

3 Links of thin core vortex rings

The first mathematical study of dynamical aspects of linked vortex rings was done by J.J. Thomson³⁶ (see also the paper by Ricca & Weber³²). His work was inspired by Kelvin's vortex atom theory, and provides one of the most remarkable examples of combination of topological ideas and fluid mechanics. Thomson's idea was to study vortex structures, linked and knotted together, by using thin core models of vortex rings and basic notions of linking, based on Gauss's formula of linking number.⁷ Thomson tackled the problem by considering a particular geometry given by two linked vortex rings lying on the mathematical surface of a torus Π of radius R and small diameter d . The simplest example of this kind of link was given by two inter-linked rings, C_1 and C_2 , embedded on Π as shown in Figure 4.

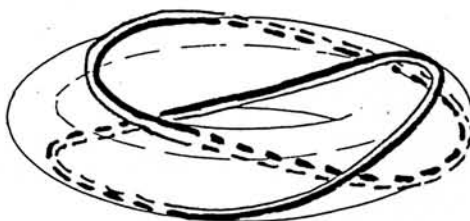


Figure 4: Simple link of two rings C_1 and C_2 , lying on the mathematical torus Π : the number of components is $n = 2$, and the linking number of the system is $Lk = 1$.

In Thomson's view the vortex link geometry is the result of the uniform, rigid rotation of two point vortices (representing the cross-sections of two vortex filaments) around their center of mass (in the meridian plane of Π), making one complete rotation around the great circle (of radius R) in the longitudinal direction. The vortex filaments were given by the collection of the point vortex positions. The resulting vortex system, made of these thin, closed vortex filaments embedded in ideal fluid, is frozen. Hence, the dynamics of the system is expected to be influenced by the type of linking.

Let $\lambda = \max |X_i - X_i^*|$, for points $\{X_i, X_i^*\} \in C_i$, $i = 1, 2$, and $\delta = \min |X_1 - X_2|$ for points $X_1 \in C_1$ and $X_2 \in C_2$. If we assume that $\lambda \gg \delta$, where $\lambda = O(2R)$ and $\delta = O(d)$, then we can show that:

Theorem (Thomson, 1883). *Consider the link formed by two vortex rings of equal circulation Φ and relative linking number Lk , embedded and equally spaced on a torus Π in \mathcal{D} . The vortex system is steady and stable iff*

$$\frac{M(2\pi\rho\Phi)^{1/2}}{LkP^{3/2}} < 1, \quad (9)$$

where ρ is the fluid density (constant) and $M = |M|$ and $P = |P|$ are the intensities of the angular momentum M , and the linear momentum P of the system.

The simplest link system (with $Lk = 1$) rotates and translates as a rigid body, with angular velocity Ω and translational velocity V given by

$$\Omega = \frac{\Phi}{\pi d^2}, \quad V = \frac{\Phi}{4\pi R} \log \frac{64R^2}{a^2}. \quad (10)$$

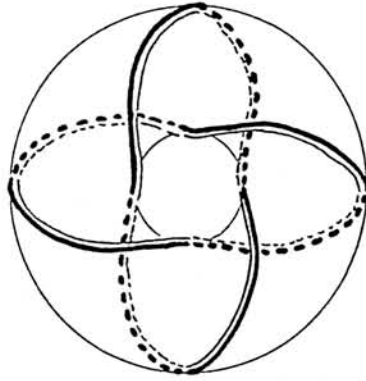


Figure 5: Example of higher-order link made of two rings: in this case $n=2$, $Lk = 2$.

Higher-order link systems (i.e. two-component link with $Lk > 1$) are realized by a higher number of full rotations of the point vortex system around the great circle (see Figure 5).

Consider now n vortex rings linked together. Following a similar construction, the n -component link is now given by n inter-linked vortices on Π (see Figure 6). The system is generated by the rigid rotation of n point vortices equally spaced on the torus small circumference. After a long and laborious analysis Thomson finds the following result:

Theorem (Thomson, 1883). *Consider the link of n vortex rings of equal circulation Φ and relative linking number Lk , embedded and equally spaced on a torus Π in \mathcal{D} . The vortex system is steady and stable iff $n \leq 6$, with period of vibration*

$$T = \frac{2\pi}{\Phi \left(\frac{2}{d^2} - \frac{(2Lk^2 - 1)}{4a^2} \log \frac{d}{a} \right)}. \quad (11)$$

This result has been confirmed by later works in the theory of point vortex motion in the plane.³³

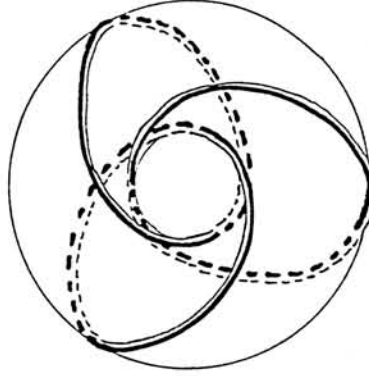


Figure 6: Example of higher-order link given by three rings on the torus Π : $n=3$ and relative linking $Lk = 1$.

4 Evolution and stability of thin vortex knots

4.1 Kelvin's conjecture and vortex knot dynamics

In his vortex atom theory, Kelvin¹⁴ conjectured (see Vortex Statics, p. 123, ¶ 16) that thin vortices in the shape of torus knots could exist as steady and stable fluid structures. Vortex knot solutions (to Euler's equations), if existed, could move with constant speed in the fluid and, if disturbed, vibrate about their equilibrium configuration. From a mathematical viewpoint the search for the existence of vortex knots remained open, and only in recent years there has been a real progress in this study. Here we want to present and discuss some new results.

Thin vortex knots have been found as solutions to the so-called 'localized induction approximation'²⁷ (LIA for short). This is an approximation of the Biot-Savart law for Euler's equations. Under LIA, vortex motion is governed by a law, that after appropriate re-scaling of the time variable, takes the simple form

$$\text{LIA : } \quad \mathbf{u} = \dot{\mathbf{X}} = \mathbf{X}' \times \mathbf{X}'' = c\hat{\mathbf{b}}, \quad (12)$$

where \mathbf{u} is the vortex velocity, the dot denotes time-derivative and the prime denotes derivative with respect to arc-length along the tube axis. c and $\hat{\mathbf{b}}$ are local curvature and unit binormal to the axis. It is interesting to note that since eq. (12) is equivalent to the non-linear Schrödinger equation,⁸ we

have a countably infinite number of polynomial conserved quantities (soliton invariants) that can be written as global geometric functionals.^{17,23}

Existence and steadiness of knotted solutions to LIA have been studied by Kida¹⁵ and Keener.¹² Kida's solutions are torus knots in the physical space and represent the first vortex knot solutions found by analytical methods. We have:

Theorem (Kida, 1981). *Let K_v denote the embedding of a knotted vortex filament in an ideal fluid in \mathcal{D} . If K_v evolves under LIA, then there exists a class of steady solutions in the shape of torus knots $K_v \equiv T_{p,q}$.*

In geometric terms Kida's solutions are closed curves embedded on the mathematical torus, wrapping the torus $p > 1$ times in the longitudinal direction and $q > 1$ times in the meridian direction (p, q co-prime integers). The winding number is given by $w = q/p$, and self-linking given by $Lk = pq$, two topological invariants of the knot type. Kida gives the solutions in terms of fully non-linear relationships that involve elliptic functions of traveling waves. A more direct and simpler approach has been proposed by Ricca,²⁵ and is based on linear perturbation techniques and cylindrical polar coordinates (r, α, z) . By this approach we find 'small-amplitude' torus knot solutions (asymptotically equivalent to Kida's solutions) given by

$$\left. \begin{aligned} r &= r_0 + \epsilon_0 k_r \sin(w\phi + \phi_0) \\ \alpha &= \frac{s}{r_0} + \epsilon_0 \frac{k_r}{wr_0} \cos(w\phi + \phi_0) \\ z &= \frac{\hat{t}}{r_0} + \epsilon_0 k_r \left(1 - \frac{1}{w^2}\right)^{1/2} \cos(w\phi + \phi_0) \end{aligned} \right\} \quad (13)$$

r_0 is the radius of the torus circular axis and $\epsilon_0 = a/r_0 \ll 1$ is the inverse of the aspect ratio of the vortex, with a the radius of the vortex cross-section and $k_r = O(r_0)$ a scale factor. Moreover $\phi = (s - \kappa t)/r_0$, with t time, \hat{t} a time re-scaled with the vortex circulation, and ϕ_0 a constant.

4.2 New results on stability of vortex knots

Since torus knots have two isotopes $T_{p,q}$ and $T_{q,p}$ (for given p and q), that are topologically equivalent but geometrically different, the question of their evolution and stability is particularly interesting. A linear stability analysis^{25,26} based on equations (13) leads to the following result:

Theorem (Ricca, 1993; 1995). *Let $T_{p,q}$ denote the embedding of a 'small-amplitude' vortex torus knot K_v evolving under LIA. $T_{p,q}$ is steady and stable*

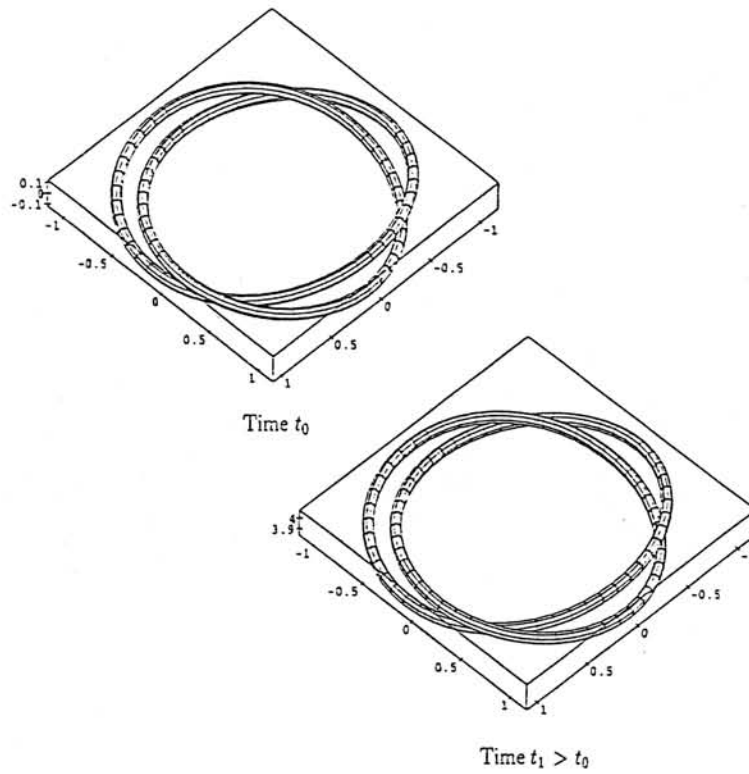


Figure 7: Evolution of torus knot $T_{2,3}$ under LIA. The knot is found to be stable as predicted by the LIA analysis of Ricca. The knot is visualized by centering a thin tube on the knot axis. The tube shown is therefore a virtual object and its thickness is not measured by a_0 .

under linear perturbations iff $q > p$ ($w > 1$).

Kelvin's conjecture can be therefore tested using this criterium. Numerical calculations^{34,31} have been performed to check and investigate the validity of the above result, and confirm that knots with winding number $w > 1$ are indeed stable under LIA evolution.

Figure 7 shows two snapshots of the stable knot $T_{2,3}$ and Figure 8 shows the knot $T_{3,2}$ as it becomes unstable and unfolds. Another interesting result³¹ is the discovery of a strong stabilizing effect due to the full Biot-Savart law. Take for example the knot $T_{3,2}$: this knot becomes immediately unstable under LIA, whereas it remains stable under Biot-Savart, travelling a considerable distance. Although we find that these knots eventually de-stabilize (remember

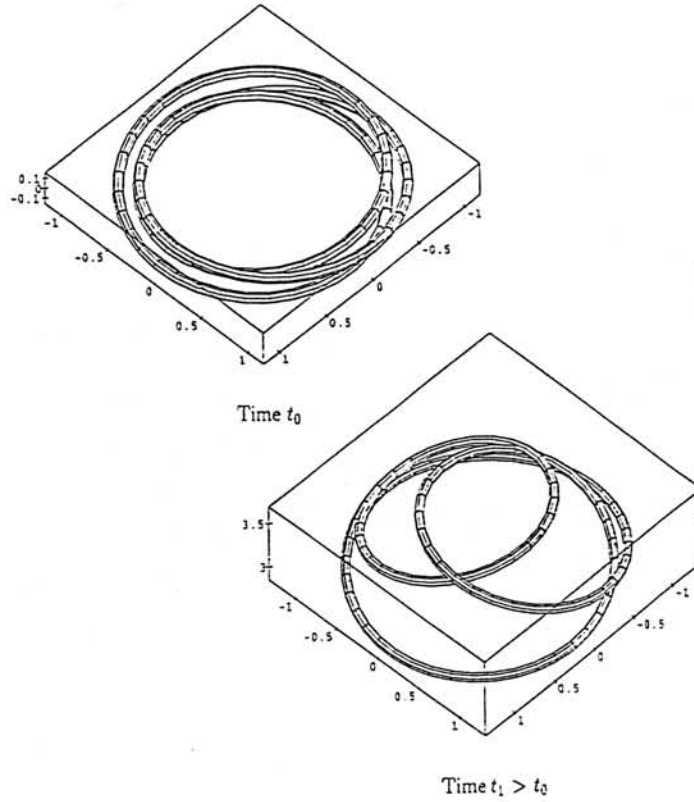


Figure 8: Evolution of torus knot $T_{3,2}$ under LIA. The knot is found to be unstable as predicted by the LIA analysis of Ricca. The knot is however stabilized when its evolution is governed by the Biot-Savart law.

that some numerical noise is always present), the time which elapses and the distance over which the knot travels before breaking-up is very large and has physical significance.

Finally, let us point out that unstable vortex knots evolve under LIA towards a reconnection event. This is another interesting feature of vortex knot evolution, especially in view of the great interest for the study of singularity formation. No doubt that these results will stimulate more numerical work and will certainly give new impetus to the mathematical search for the existence of steady and stable vortex knot solutions under the Euler equations.

5 Magnetic knots, minimal braids and energy estimates

5.1 Evolution of inflexional magnetic knots

Magnetic knots are the physical analog of vortex knots, when we replace vorticity with the magnetic field (so that the physical knot becomes a magnetic flux tube). Magnetic knots evolve according to a dynamics given by the Lorentz force. For a solenoidal magnetic field $\mathbf{B} = \mathbf{B}_m + \mathbf{B}_a$ given by a meridian (i.e. poloidal) component \mathbf{B}_m and an axial (i.e. toroidal) component \mathbf{B}_a , where

$$\mathbf{B}_m = [0, B_\theta(r, \vartheta(s)), 0], \quad \mathbf{B}_a = [0, 0, B_s(r)], \quad (14)$$

with B_θ and B_s smooth functions of radius of the tube cross-section r ($0 \leq r \leq a$) and azimuth angle $\vartheta = \vartheta(s)$ ($0 \leq \vartheta \leq 2\pi$; s arc-length on the tube axis), we have²⁸

$$\mathbf{F}_\perp = B_s^2 \frac{c}{K} \hat{\mathbf{n}} - \left[\frac{B_\theta^2}{r} + \frac{1}{2} \frac{\partial}{\partial r} (B_\theta^2 + B_s^2) \right] \hat{\mathbf{e}}_r, \quad (15)$$

where \mathbf{F}_\perp denotes the component of the force perpendicular to the tube axis. Here K is a scale factor (function of the geometry), and $\hat{\mathbf{n}}$ and $\hat{\mathbf{e}}_r$ are two unit vectors in the principal normal direction and in the radial direction to the tube axis. Since \mathbf{F}_\perp is the only component of the force responsible for the motion of the knot in the fluid, in a first approximation we can write $\mathbf{F} \approx c\hat{\mathbf{n}}$, with force proportional to curvature, along the principal normal of the knot axis. This force induces a tension in the physical knot and a shortening of the lines of force.

In general magnetic knots exhibit inflexional configurations. The geometry of these configurations is characterized by a change in concavity in the tube axis, at a point where curvature vanishes (inflexion point). Inflexional states are easily identified in plane curves: in this case the inflexional geometry is simply given by an *S*-shaped curve with the inflexion point at the change of concavity. Inflexional configurations in magnetic field structures, however, are ubiquitous, especially in rich topologies. Moffatt & Ricca²⁴ showed that the appearance of inflexional states is invariably associated with the continuous exchange of writhe and twist (see Figure 9), a natural mechanism in the evolution of magnetic structures.

The dynamics of magnetic flux tubes in inflexional configuration has been studied by applying the Lorentz force equations to a generic deformation through inflexion. It can be shown²⁸ that inflexional states represents disequilibria for magnetic configurations. In particular we can state the following result.²⁹

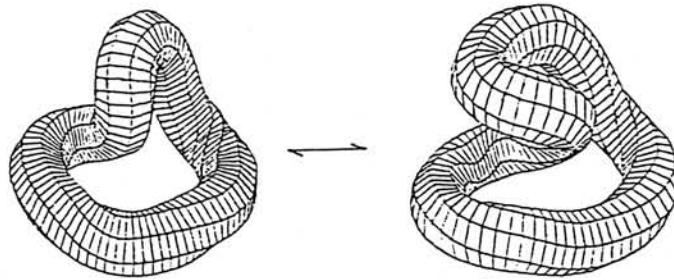


Figure 9: Competition between twist and writhe in a magnetic knot.

Theorem (Ricca, 1997). *Let K_m be the embedding of a magnetic knot in \mathcal{D} . If K_m has a finite number of inflexion points in isolation, then K_m evolves to an inflexion-free configuration, possibly in braid form.*

As we shall see below this result has important consequences for the first stages of the relaxation of magnetic knots.

5.2 Relaxation of inflexional knots to minimal braids

Since inflexional magnetic knots are in disequilibrium, they remove inflexions by re-arranging the geometry to form topologically equivalent configurations free from inflexions. In general the Lorentz force induce a natural tendency to minimize the magnetic tension present in the tube by reducing the surplus of internal magnetic twist (through an increase of writhing), and by removing inflexion points. This favours a deformation to topologically equivalent inflexion-free configurations. In absence of other forces, the evolution is then dominated by curvature forces that induce a continuous, progressive shortening of the field lines (hence of the knot) toward a minimum energy state. In the ideal process, virtual crossings and inflexional states are naturally removed and the knot relaxes isotopically to an inflexion-free configuration, with least possible number of (real) crossings ('minimal closed braid form'; see Figure 10). In general this number of crossings is equal to, or higher than, the topological crossing number.

Minimal braids are particular geometric representations of knot types. From a purely topological viewpoint, any knot can be isotoped to a closed braid by a sequence of Reidemeister's moves (in braid theory this result is

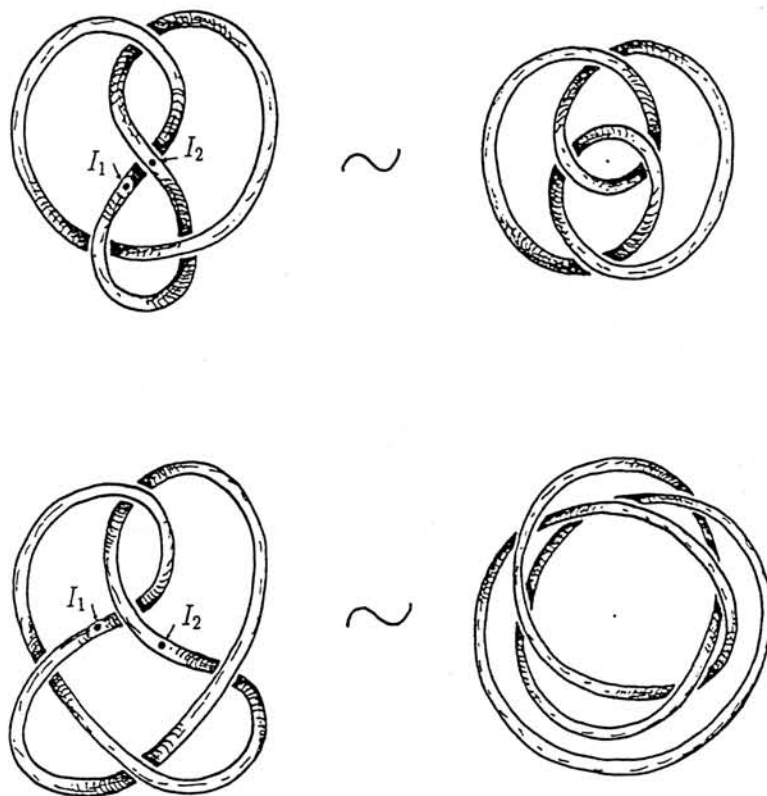


Figure 10: Two different knot types are shown in standard, minimal projection (on the left hand side) and in their topologically equivalent minimal, closed braid form (on the right hand side). Note that the knots in their standard representation exhibit at least two points of inflexion, denoted by I_1 and I_2 in the diagram. These knots can be both isotoped to their minimal closed braid representation, which is given by an inflexion-free configuration with the least possible number of crossings.

known as Markov's theorem⁴). The deformation of an inflexional knot into a closed braid representation (as is given in the 'conjugacy class' of the knot type) is likely to introduce new crossings. To see this, let us consider the two examples of isotopic transformation of knotted loops shown in Figure 10. The diagrams on the left show two different knot types in minimal projection, i.e. in the plane projection for which the number of crossings is the topological crossing number C_{\min} . In this configuration the knots have at least two points of inflexions (denoted by I_1 and I_2 in the diagrams; note that inflexional states are intrinsic geometric features independent of projection angle and viewing direction). The corresponding diagrams on the right, however, show no points of inflexions, and represent the isotopic configurations of the knots in the minimal braid form, with curvature vector pointing always inward the braid region. Note that in passing from the minimal standard to the minimal braid configuration the four crossing knot conserves the minimum number of crossings ($C_{\min} = C_0 = 4$), whereas the five crossing knot (with $C_{\min} = 5$) has the least possible number of crossings $C_0 = 6 > C_{\min}$. In general we have $C_0 \geq C_{\min}$. Our analysis,²⁹ based on standard results of knot theory,^{19,37} shows that indeed there are infinitely many knots (whose simplest representative is the five-crossing knot) that cannot be transformed to minimal braids by 'equi-minimal' isotopies (i.e. by conserving the minimum possible number of crossings). The existence of a family of knots that have 'non-equi-minimal' braid representatives seem to have important consequences for the estimates of energy minima of magnetic knots.

5.3 Possible consequences for energy estimates

Mathematical estimates of minimum energy levels based on topological information have shown^{21,63,29} that minimum energy states of physical knots can be related to topological quantities such as linking number and crossing number. Lower bounds for energy levels of magnetic knots are given by relations of the kind

$$E_{\min} \geq f(\Phi, V, n, C_{\min}), \quad (16)$$

where E_{\min} denotes the ground state energy and $f(\cdot)$ gives the relationship between physical conserved quantities — such as total flux Φ , magnetic volume V , number of tubes n (in the case of an n -component braid or link) — and topology (here given by C_{\min}). Typically, in these relations energy increases with knot complexity. The inequality sign allows ample margins for errors, so that these estimates are still rather qualitative. For inflexional magnetic knots, far from their minimum energy state, our results indicate that ground energy levels may be strongly influenced by the presence of inflexions. Since inflexions

represents disequilibria of thin magnetic knots, inflexional knots will tend to remove inflexions and relax to minimal braids first, before relaxing further to their ground energy state. But minimal braids are likely to have least possible number of crossings $C_0 > C_{\min}$ (as for the five-crossing knot of Figure 10). For this sub-family of minimal braids ('non-equi-minimal' braids) we expect an E_{\min} higher than the theoretical bound given by the equality sign in (16).

This studies find useful applications in applied disciplines, such as astrophysics, solar physics and fusion plasma physics. For solar coronal loops, for example, a difference in the crossing number of the relaxing magnetic braid has important physical consequences for energy estimates, especially when these estimates are based on theoretical models that are very sensitive to variations in geometric and topological information. The accuracy of these estimates is crucial to give precise evaluations of the amount of energy that can be released into heat during flares and microflares. Future progress in this direction will be very important for energy studies.

Acknowledgments

The author would like to acknowledge financial support from The Leverhulme Trust (UK) and from ISIS-JRC, Ispra (EC).

References

1. Arnold, V.I. 1974 In *Proc. Summer School in Differential Equations*. Acad. Sci. Armenian S.S.R., Erevan (in Russian). [(1986) *Sel. Math. Sov.* 5, 4, 327-345].
2. Batchelor, G.K. 1967 *An Introduction to Fluid Dynamics*. Cambridge University Press.
3. Berger, M.A. 1993 *Phys. Rev. Lett.* 70, 705-708.
4. Birman, J.S. 1976 *Braids, links and mapping class group*. Annals of Math. Studies 82, Princeton University Press.
5. Epple, M. 1998 *Math. Intelligencer* 20, 45-52.
6. Freedman, M.H. & He, Z.-X. 1991 *Ann. Math.* 134, 189-229.
7. Gauss, C.F. 1833 In *Works*. Königichlen Gesellschaft der Wissenschaften zu Göttingen, (in German).
8. Hasimoto, H. 1972 *J. Fluid Mech.* 51, 477-485.
9. Helmholtz, H. 1858 *J. Reine Angew. Math.* 55, 25-55 (in German).
10. Jones, V.F.R. 1987 *Ann. Math.* 126, 335-388.
11. Kauffman, L.H. 1987 *On Knots*. Annals Study 115, Princeton University Press.

12. Keener, J.P. 1990 *J. Fluid Mech.* **211**, 629–651.
13. Kelvin, Lord (Thomson, W.) 1867 *Phil. Mag.* **33**, 511–512.
14. Kelvin, Lord (Thomson, W.) 1875 *Proc. Roy. Soc. Edinb.* ss. 1875–76, 115–128.
15. Kida, S. 1981 *J. Fluid Mech.* **112**, 397–409.
16. Lamb, Sir H. 1879 *Hydrodynamics*. Cambridge University Press.
17. Langer, J. & Perline, R. 1991 *J. Nonlin. Sci.* **1**, 71–93.
18. Lichtenstein, L. 1929 *Grundlagen der Hydromechanik*. Verlag, Berlin.
19. Maxwell, J.C. 1873 *A Treatise on Electricity and Magnetism*. MacMillan & Co., Oxford.
20. Moffatt, H.K. 1969 *J. Fluid Mech.* **35**, 117–129.
21. Moffatt, H.K. 1990 *Nature* **347**, 367–369.
22. Moffatt, H.K. 1992 In *Topological Aspects of the Dynamics of Fluids and Plasmas* (ed. H.K. Moffatt et al.). Kluwer, Dordrecht, The Netherlands.
23. Moffatt, H.K. & Ricca, R.L. 1991 In *The Global Geometry of Turbulence* (ed. J. Jiménez). NATO ASI B **268**, Plenum Press, New York.
24. Moffatt, H.K. & Ricca, R.L. 1992 *Proc. R. Soc. Lond. A* **439**, 411–429.
25. Ricca, R.L. 1993 *Chaos* **3**, 83–91 [1995 Erratum. *Chaos* **5**, 346].
26. Ricca, R.L. 1995 In *Small-Scale Structures in Three-Dimensional Hydro and Magnetohydrodynamics Turbulence* (ed. M. Meneguzzi et al.). Lecture notes in Physics **462**. Springer-Verlag.
27. Ricca, R.L. 1996 *Fluid Dyn. Res.* **18**, 245–268.
28. Ricca, R.L. 1997 *Solar Physics* **172**, 241–248.
29. Ricca, R.L. 1998 In *Knot Theory* (ed. V.F.R. Jones et al.). Institute of Mathematics **42**, Polish Academy of Sciences, Warszawa.
30. Ricca, R.L. & Berger, M.A. 1996 *Phys. Today* **49**, 24–30.
31. Ricca, R.L., Samuels D.C. & Barenghi C.F. 1998 In *Proc. VII European Turbulence Conference* (ed. U. Frisch). Kluwer, Dordrecht, The Netherlands.
32. Ricca, R.L. & Weber, C. 1998 In preparation.
33. Saffman, P.G. 1992 *Vortex Dynamics*. Cambridge University Press.
34. Samuels, D.C., Barenghi, C.F. & Ricca, R.L. 1998 *J. Low Temp. Physics* **100**, 509–514.
35. Tait, P.G. 1898 In *Scientific Papers*. Cambridge University Press.
36. Thomson, J.J. 1883 *A Treatise on the Motion of Vortex Rings*. Macmillan & Co., London.
37. Vogel, P. 1990 *Comment. Math. Helvetici* **65**, 104–113.